2-2016

Robust Non-Permanent Magnet Motors for Vehicle Propulsion

Tsarajidy Raminosoa
Electrical Machines Laboratory

David A. Torrey
Electrical Machines Laboratory

Ayman M. El-Refaie
Marquette University, ayman.el-refaie@marquette.edu

Di Pan
Electrical Machines Laboratory

Stefan Grubic
Electrical Machines Laboratory

See next page for additional authors

Robust Non-Permanent Magnet Motors for Vehicle Propulsion

Tsarajidy Raminosoa
GE Global Research, Electrical Machines Laboratory, Niskayuna, New York, USA
David A. Torrey
GE Global Research, Electrical Machines Laboratory, Niskuyana, New York, USA
Ayman El-Rafaie
GE Global Research, Electrical Machines Laboratory, Niskayuna, New York, USA
Di Pan
GE Global Research, Electrical Machines Laboratory, Niskayuna, New York, USA
Stefan Grubic
GE Global Research, Electrical Machines Laboratory, Niskayuna, New York, USA
Kevin Grace
GE Global Research, Electrical Machines Laboratory, Niskayuna, New Yorks, USA

Abstract:

There has been growing interest in electrical machines that reduce or eliminate rare-earth material content. Traction applications are among the key applications where reducing cost and hence reduction or elimination of rare-earth materials is a key requirement. This paper will assess the potential of three non-permanent magnet options in the context of vehicle propulsion applications: 1) a conventional Switched Reluctance Machine (SRM), 2) a DC-biased Reluctance Machine (DCRM) and, 3) a Wound Field Flux Switching Machine (WFFSM). The three machines were designed to achieve the hybrid vehicle traction requirements of 55kW peak and 30kW continuous over a speed range going from 2800rpm to 14000rpm. Their performance will be compared and the key opportunities and challenges will be highlighted. Preliminary experimental results for the DCRM will be presented.

SECTION I. Introduction

Important global efforts are currently underway toward developing more environmentally friendly transportation. Development of electric and hybrid vehicles are a key part of this global effort. In order to ensure marketability of hybrid or electric vehicles, their cost has to be reduced while keeping their performance high. One impactful method is to stabilize and reduce the cost of the electrical machine by reducing or eliminating the use of rare-earth elements [1], [2] - present in permanent magnet materials - which have been experiencing significant increases and volatility in their prices.

Therefore, electrical machine topologies such as switched reluctance machines (SRMs) would be a cost effective solution due to their simplicity, mechanical robustness and lack of permanent magnets [3]. However, their application represents a number of system-level challenges that are not adequately addressed by their advocates. These challenges include torque ripple, acoustic noise, and use of a non-standard inverter topology [4]. Recently, research work was carried out on doubly salient electrical machines sharing the robustness and simplicity of SRMs and trying to address the aforementioned challenges. Those machines include DC biased Reluctance Machines (DCRM) and Wound Field Flux Switching Machines (WFFSM). Both the DCRM and the WFFSM have a DC field winding and an AC three phase armature winding. They use a conventional three phase inverter for the armature and an additional DC/DC converter for the field winding.

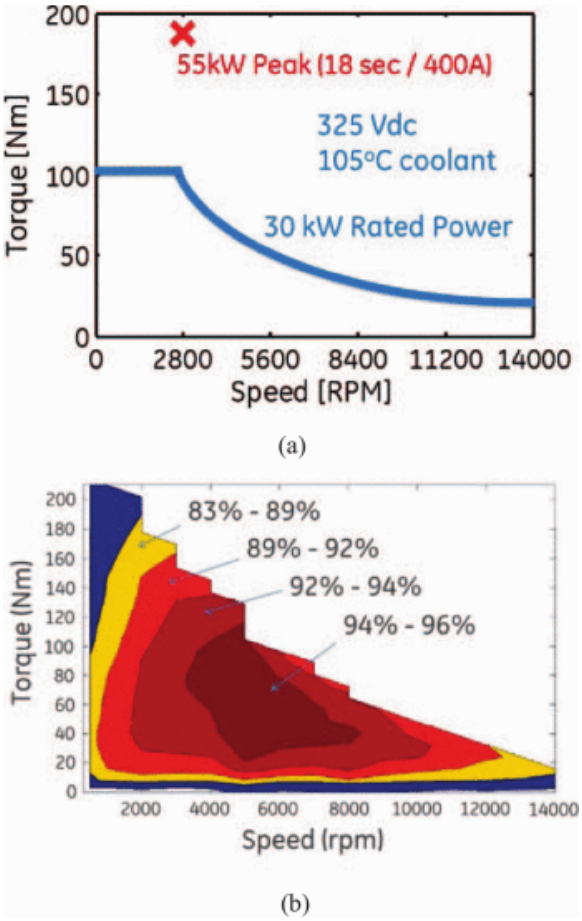

Fig. 1. Freedomcar 2020 motor specified torque-speed curve (a) and efficiency map (b).

Table I. Freedomcar 2020 advanced motor performance requirements

Requirement	**Target**	**Condition**
Minimum top speed	14,000 rpm	
Peak output power	55 kW for 18sec	at 20% speed and nominal voltage
Continuous output power	30 kW	at 20~100% speed and nominal voltage
Weight	≤ 35 kg	
Operating DC bus voltage	200~450V, 325V nominal	
Maximum phase current	400Arms	
Line-to-line Back-EMF	< 600V peak	at 100% speed
Torque pulsation	< 5% peak torque	at any speed
Coolant inlet temperature	105□C	

Table II. Active material masses

Machine Type	**SRM**	**DCRM**	**WFFSM**
Stator Iron Mass (kg)	19.5	17.7	20.3
Rotor Iron Mass (kg)	7.2	9.1	8.5
Total Iron Mass (kg)	26.6	26.8	28.8
Field Copper Mass with End Winding (kg)	0	10.5	5.4
Armature Copper Mass with End Winding (kg)	7.4	3.3	3.3

Total Copper Mass (kg)	7.4	13.8	8.7
Machine Active Mass (kg)	**34.0**	**40.6**	**37.5**

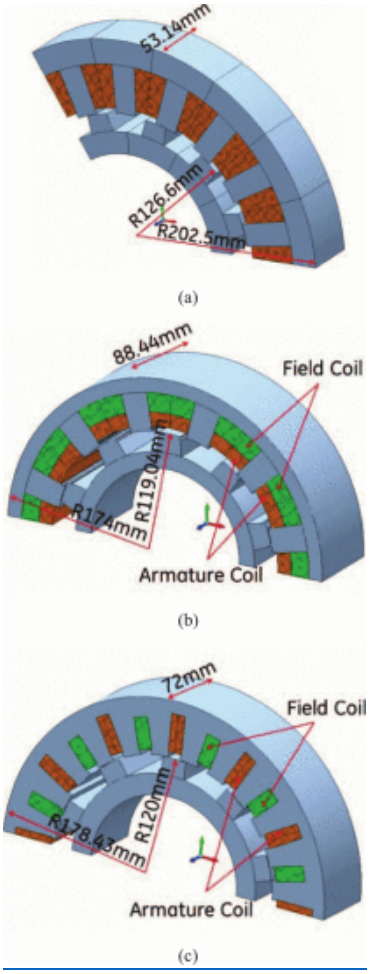

Fig. 2. Cross sections of the non-permanent magnet machines considered: (a) Conventional switched reluctance machine (SRM); (b) DC biased reluctance machine (DCRM); (c) wound field flux switching machine (WFFSM).

This paper compares the performance of a conventional SRM, a DCRM and a WFFSM designed to achieve the hybrid vehicle traction requirements of 55kW peak and 30kW continuous over a speed range going from 2800rpm to 14000rpm under the Advanced Non Rare Earth Electrical Machine Program funded by the US Department of Energy. The specifications are summarized in Fig. 1 and Table I.

SECTION II. Opportunities and Challenges of the Proposed Non-Permanent Magnet Options

The operating principle and Feasible slots/poles combinations of Wound Field Flux Switching Machines and Sinusoidal Reluctance Machine with DC winding were presented and analyzed by others [1], [5]. In this work, we selected an 18 slot 12 pole conventional SRM, a 12 slot 10 pole DCRM and a 24 slot 10 pole WFFSM and designed them for best specific torque. The three robust non-permanent magnet options can offer many attractive opportunities for traction applications, but they come with some challenges as described below.

A. Opportunities

- DCRM and WFFSM have inherently lower torque ripple than the Conventional SRM.
- DCRM and WFFSM can be driven with a conventional three phase AC drive and a separate auxiliary DC/DC converter with decoupled control of the DC excitation that can help extend the speed range. It should be noted that the DC/DC converter is sized to support only the copper losses in the field winding estimated to be 2.9kW under peak power operation.
- The design space for the DCRM is opened to other stator/rotor pole combinations that would not be FEAsible for a Switched Reluctance Machine (12s/10r, for example).
- The three machines are simple, robust, and have no rotor windings or permanent magnets.
- DCRM and WFFSM have smooth Back-EMF and low cogging torque and torque ripple for suitable stator/rotor pole combinations. Minimization of torque ripple is straightforward.
- The DCRM is similar to the conventional SRM, uses tooth windings which provide advantages in terms of machine overall length, size as well as ease of manufacturing.

B. Challenges

The three machines considered are inherently high pole count machines and operate at high fundamental frequencies. At 14000rpm, the DCRM and WFFSM with 10 rotor poles (i.e. 10 pole pairs) operate at 2.3kHz while the fundamental frequency of the SRM with 12 rotor poles is 2.8kHz. Most of the challenges are related to the high frequency nature of the machines.

- Iron loss: The stator and rotor laminations are experiencing high frequency variation of flux density causing the iron losses to grow quickly with the speed. This poses a special challenge in the rotor and requires special consideration in the present application. To tackle the iron losses, thin gauge lamination material (down to 10mil (0.00in) or lower) may be necessary. The l 0mil laminations used are commercially available in a widespread manner and do not represent any significant additional cost compared to other silicon steel lamination grades/thicknesses.
- AC losses in windings: Due to the high fundamental frequency at top speed, some type of Litz wire was necessary for the three phase windings in order to reduce the strand induced eddy current and circulating current losses. In the DCRM, the field winding is collocated with the armature winding and therefore experiences AC losses too. Hence, the wire size has to be carefully chosen but Litz wire can be avoided. Even though the use of Litz wire adds cost, this is more than offset by the cost reduction achieved by eliminating permanent magnets. The use of Litz wire limits slot fill, increasing the size of the machine.
- Control:
    - DCRM and WFFSM: An elaborate control strategy making a transition from asynchronous PWM to synchronous PWM and ultimately to six-step voltage control at high speed is necessary to ensure controllability up to the 2.3kHz fundamental frequency. Partitioning control between the field and armature windings requires careful consideration.
    - Conventional SRM: requires a non-standard half-bridge inverter per phase. The control of the turn ON and turn OFF angles at high speeds are challenging. Further, there is opportunity to control torque ripple only below base speed.
- Friction and windage losses: Since these are high-speed machines with salient pole rotors, friction and windage losses can be significant at high speeds. Measures have been taken to smooth out the rotor surface to minimize these losses as will be discussed in Section V.

SECTION III. Comparison Basis

The three machines were designed for the same set of specifications and under the same design constraints, including an airgap of 0.73mm, a maximum RMS current density of 20A/mm^2 in copper for the peak torque operation and 10A/mm^2 for continuous torque. The AC losses were estimated using the method described in [1] and were included in the performance calculation. Litz wire was used in the armature windings, leading to a relatively low fill factor of 27.5%. In addition, a 5mm recess of the armature conductors from the airgap was found to further minimize the AC losses and was applied to the three designs. The field winding carries a DC current but still experiences some degree of AC losses induced by the airgap fringing field (WFFSM) or by the armature winding when sharing the same slots (DCRM). However, we found that regular conductors with a suitable gauge can be used and a fill factor of 55% can be achieved. Cross sections of the three machines are shown in Fig. 2.

The performance of the three machines is evaluated at four representative operating conditions: Peak power at 2800rpm, Corner point rated power at 2800rpm, rated power at 8400 rpm and 14000rpm. For the WFFSM and DCRM, several operating points with various field excitation levels are possible for a given set of power and speed. Hence, the operating points were optimized in order to maximize the efficiency. Flux Maps were generated for several levels of field excitation. For each level of excitation, the MTP A operating points were calculated. Figure 3 shows the efficiency of the MTP A operating points against the field excitation level for the DCRM. Figure 4 shows the efficiency against the field excitation for the WFFSM. For each representative operating condition, the field excitation level providing the highest efficiency was selected as the optimal operating point. One observation from Figures 3 and 4 is that at high speed, the maximum efficiency operating point corresponds to the lowest field excitation current that is able to provide the required power. In fact, choosing the lowest possible field sets the flux density level in the laminations to its lowest level, lowering the iron losses which are dominant at high speed. At low speed, although the copper losses are the most significant, the iron losses are important enough to affect the efficiency. Hence, there is an optimum field excitation that maximizes the efficiency.

For the conventional SRM, the turn-ON and turn-OFF angles and the reference currents were calculated using single phase voltage driven simulations for a given speed. The current waveforms were determined from a voltage driven simulation using an asymmetric half bridge and a 325V DC bus. At low speed, the current rising slope is obtained by applying the full DC bus voltage at the turn-ON time. The current is then maintained constant once reaching the reference current. In an actual set-up, the current controller will maintain the current at this reference current. The full DC bus voltage is applied with a reversed polarity at the turn-OFF time to make the current fall to zero. At high speed, there is no constant plateau of the current (no current control). Only one phase is considered in the voltage driven simulation to keep the simulation time reasonable. The obtained steady state current waveform is used for the re-constitution of the three phase currents which are re-inj ected as current sources in a current driven simulation to evaluate SRM performance. In this way, the mutual interactions among phases - which are generally negligible - are considered. Figure 5 shows current waveforms used for the four representative operating points. It can be seen that the current waveforms are realistic and will provide an accurate assessment of the torque ripple.

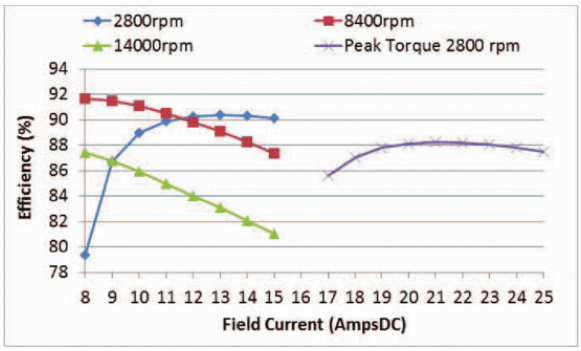

Fig. 3. DCRM operating point optimization to maximize efficiency.

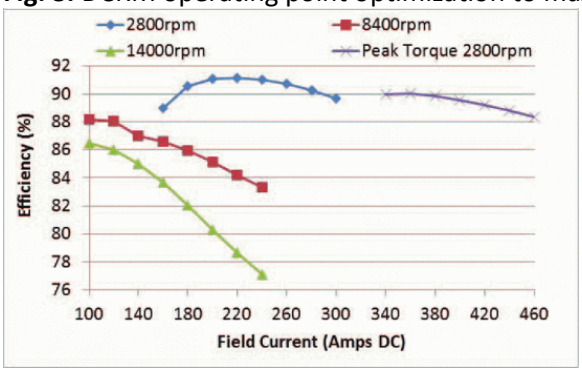

Fig. 4. WFFSM operating point optimization to maximize efficiency.

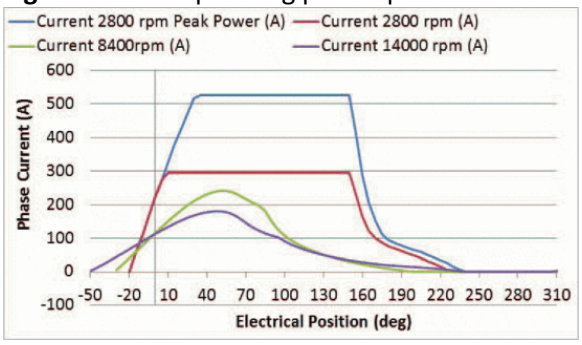

Fig. 5. SRM current waveforms for four representative operating points.

SECTION IV. Performance Comparison and Discussion

The three designs are able to provide the required peak and continuous power within the current and voltage limitations. The active material masses are summarized in Table II. The conventional SRM offers the most attractive power density with 34kg active mass, followed by the WFFSM with 37.5kg active mass. The DCRM shows the highest mass with 40.6kg. The iron utilization is rather similar in the three designs, with the WFFSM using slightly more. The most significant difference is on the copper utilization: the conventional SRM is using the least copper (7.4 kg), followed by the WFFSM (8.7 kg). The DCRM is using the most copper with 13.8 kg copper mass. This will be explained later in this section.

Figure 6 compares the open circuit phase back EMF in the DCRM and WFFSM at the corner point excitation level. Both wound field machines exhibit a smooth back EMF and a very low cogging torque (Fig. 7). It should be noted that the higher back EMF magnitude in the DCRM is not necessarily an indication of higher power density but the result of different number of turns per phase between the two designs. Also, the balance between field and armature excitation levels is not identical between the two machines. The DCRM uses lower armature current than the WFFSM to achieve the required peak torque, as can be seen in Fig. 8.

Figure 9 shows the torque waveforms of the three machines when providing peak average torque. Both the DCRM and WFFSM have a very smooth torque while the SRM exhibits high torque ripple. At low speed, some reduction in the SRM torque ripple is possible through current profiling as described in [6].

Figure 10 shows the copper loss in the three designs for various speeds. Figure 11 shows the copper loss split between field and armature winding for the DCRM and WFFSM. Figure 12 shows the iron losses, and Fig. 13 the efficiency. According to Fig. 13, the efficiencies of the three designs are over 90% at the corner point, with the WFFSM exhibiting the highest. The efficiency of the WFFSM falls rapidly with the speed and is the lowest in the high speed range. The conventional SRM has the highest efficiency in the high speed range. The trends observed in the copper losses, iron losses and efficiencies will be explained in the following paragraphs.

Figure 14 shows the excursions of the flux density in the stator back iron of the WFFSM and DCRM for a field copper loss of 2500W - close to the optimal excitation levels for peak torque operation - and with open circuit three phase winding.

In the WFFSM, the flux density in the portion of stator back iron above an armature slot is bipolar, and takes advantage of a wide and mostly linear swing between the 1 st and 3rd quadrant (Fig. 14). It is unipolar above a field slot. In both cases, the effect of the saturation on the extreme positive and negatives values are moderate.

In the DCRM, the stator back iron flux density is unipolar and swings only within one quadrant. An important part of its excursion is located in the high saturation area (Fig. 14). Hence, for the same field excitation investment, the DCRM is significantly more affected by saturation than the WFFSM because of the limited excursion available to the flux density. This explains why the DCRM requires higher copper losses to achieve the same output peak torque (Fig. 10 and 11). The significant effect of the saturation in the DCRM also requires higher Amp-turns to magnetize the back iron. Therefore, higher copper content is required in the field winding of the DCRM to keep the copper losses viable under peak torque operation (Table II: 10.5kg of copper needed in the field winding of the DCRM vs. 5.4kg in the WFFSM).

Figure 15 shows the excursion of the flux density in the stator back iron of the WFFSM and DCRM under peak torque operation including the effect of the armature excitation. It can be seen that the armature contributes in further saturating the back iron in both wound field machines. However, the saturated portion of the flux density excursion is wider in the DCRM. The lower significance of the saturation in the WFFSM reduces the overall excitation requirement and leads to lower copper losses and higher efficiencies at low speeds (Fig. 10 and 13).

The above observations highlight that the unipolar nature of the flux density in the DCRM and the associated limitation of the excursion available to the flux density is an inherent disadvantage that limits its overload capability compared to the WFFSM.

As to the iron losses, at low speeds, they are similar in the three designs (Fig. 12). At high speeds, the WFFSM exhibits significantly higher iron losses than the two other designs, while the SRM shows the lowest iron losses.

At high speeds, both the DCRM and WFFSM operate in the linear region of the lamination magnetic characteristics as shown in Fig. 16(a). In the WFFSM, the flux density in the portion of stator back iron above the armature slot is bipolar, and has a wide excursion between negative and positive extremes. The flux density in the portion of stator back iron above a field slot is unipolar and the excursion is limited within one quadrant. In the DCRM, the flux density in the stator back iron is always unipolar with the excursion limited to one quadrant. The wide excursion of the flux density in half of the WFFSM back iron contributes to higher hysteresis (wider hysteresis loop area) and higher lamination eddy currents (higher amplitude of the flux density, and

consequently of its derivative) at high speed. This is why the iron loss in the WFFSM is significantly higher at high speeds.

The bipolar nature of the flux density is an advantage for the WFFSM for low speed operation where the copper losses are dominant. The wider flux density excursion increases its torque capability and improves its low speed efficiency. The same wider flux density excursion is a disadvantage at high speed where the iron losses are dominant. At high frequencies, the wider flux density excursion significantly increases the iron losses (both hysteresis and eddy current losses) in the WFFSM and deteriorates its high speed efficiency (Fig. 13).

The stator of the SRM also sees mostly unipolar flux density. In addition, the SRM is naturally field weakening in high speed, so the magnitude of the flux density is lower than in the DCRM, as can be seen in Fig. 16(b). It should be noted that, unlike in the DCRM and WFFSM, the flux density waveforms in three adjacent portions of the SRM stator back iron are not symmetrical since asymmetric excitation configuration was used [7]. In the SRM, the flux density excursions are shorter than in the DCRM in all three portions of the stator back iron. In one portion, the flux density has a significantly lower magnitude than in the two others (Fig. 16(b)). Hence, at high speeds, the iron losses in the SRM are lower than in the DCRM, despite the frequency of the stator flux density being higher in the SRM (2.8kHz in the SRM vs. 2.3kHz in the DCRM) (Fig. 12). As a result, the SRM is significantly more efficient at high speeds (Fig. 13).

Apart from mass and the electromagnetic performance, manufacturing considerations favor the SRM and DCRM as their windings are tooth wound, thereby simplifying the winding process and potentially improving the fill factor. In the WFFSM, the field and armature windings overlap which makes the winding layout challenging to manufacture.

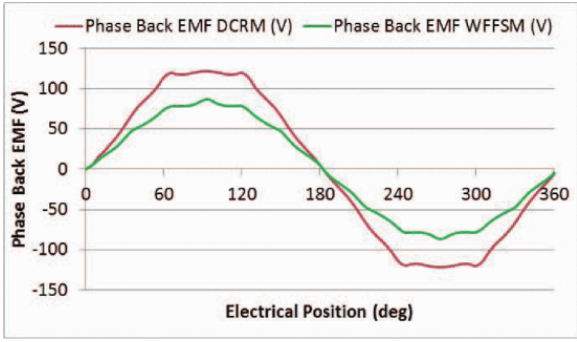

Fig. 6. Open circuit phase back EMF at corner point excitation.

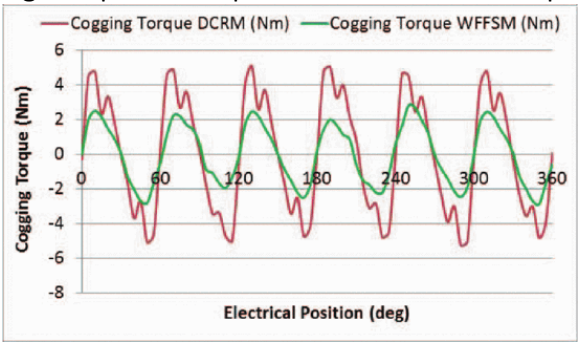

Fig. 7. Cogging torque at corner point excitation.

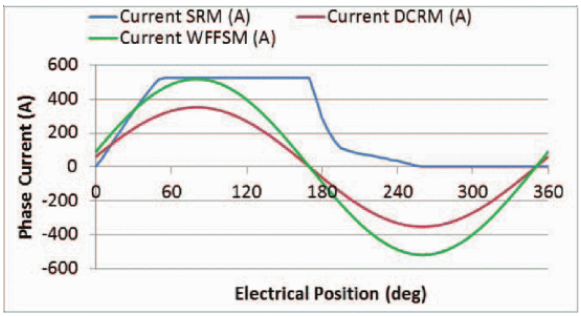

Fig. 8. Phase current waveforms under peak torque operation.

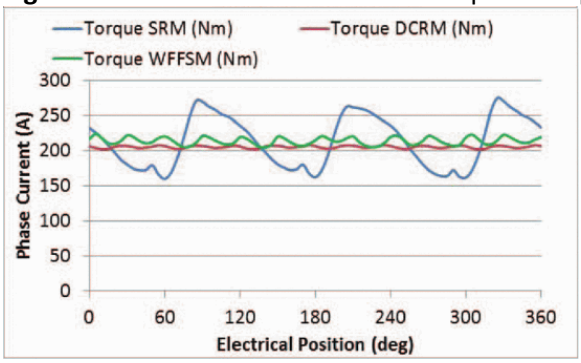

Fig. 9. Peak torque waveforms.

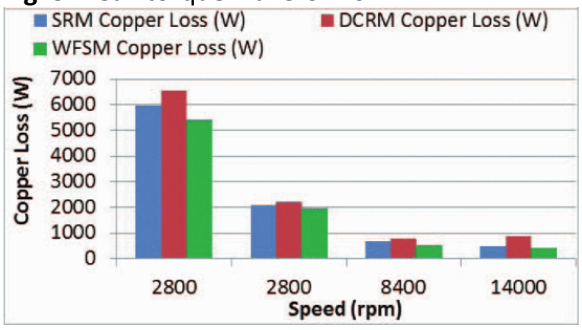

Fig. 10. Copper losses.

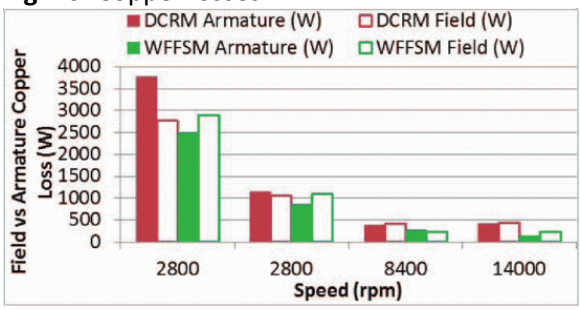

Fig. 11. Copper loss split between field and armature winding.

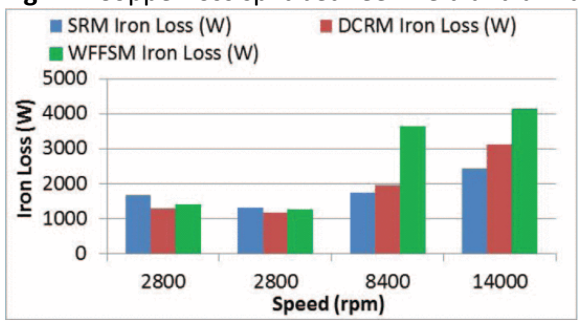

Fig. 12. Iron losses.

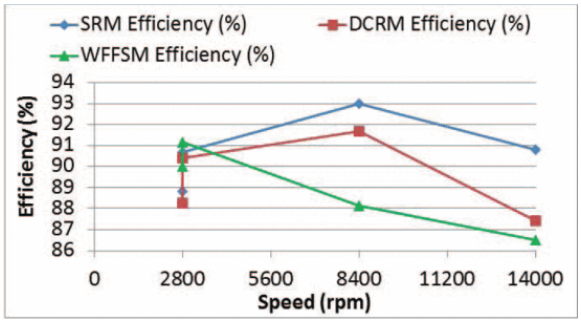

Fig. 13. Efficiency.

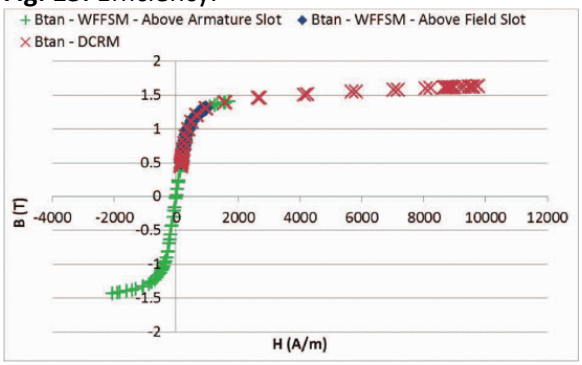

Fig. 14. Excursions of the flux density in the stator back iron of the DCRM and WFFSM under 2500W field excitation losses and open circuit armature winding.

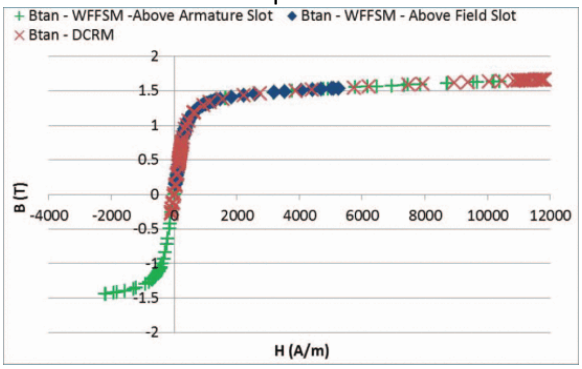

Fig. 15. Excursions of the flux density in the stator back iron of the DCRM and WFFSM under peak torque operation.

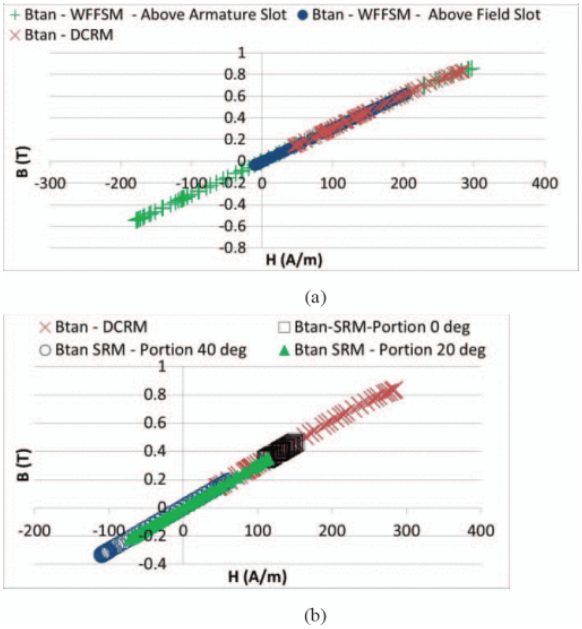

Fig. 16. Excursions of the flux density in the stator back iron under operation at top speed: (a) DCRM vs. WFFSM, (b) SRM vs. Dcrm.

SECTION V. Prototype Build and Preliminary Test Results

A 12 slot 10 pole DC Biased Reluctance Machine prototype was built and testing initiated. Fig. 1 7 (a) shows the stator while Fig. 1 7 (b) shows the rotor. As shown in Fig. 17(b), non-magnetic composite wedges were used to fill the interpolar rotor spaces and smooth the rotor surface to reduce friction and windage losses at 14,000 rpm. Figure 18 shows the predicted and measured open circuit phase voltage waveforms. Figure 19 shows the predicted and measured back EMF constant as function of the DC field current. Figure 20 shows the predicted and measured torque as function of the phase current for two levels of field excitation corresponding to peak torque (21Amps DC) and corner point (13Amps DC) operations. The measured peak torque is 8.6% lower than prediction. This is mainly due to three-dimensional effects since 7% torque discrepancy was calculated between 2D and 3D FE analyses. It should be noted that the machine is able to provide the required 187.6Nm peak torque.

Overall, there is a good agreement between FE predictions and measurements.

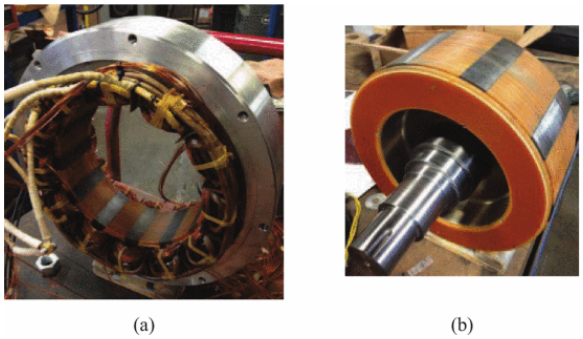

Fig. 17. Prototype photographs: (a) Stator; (b): rotor.

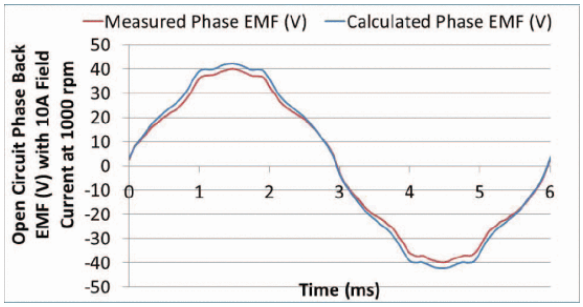

Fig. 18. Measured vs. Calculated open circuit phase voltage for 10amps DC field current and 1000rpm.

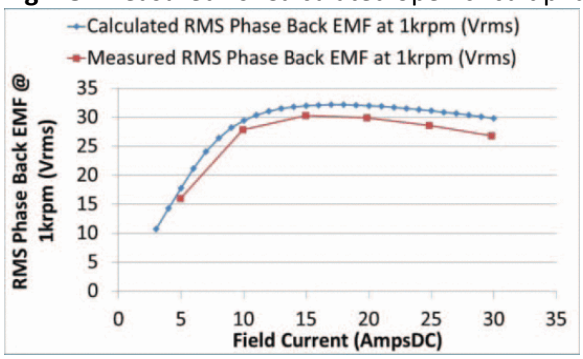

Fig. 19. Measured vs. Calculated RMS phase back EMF at 1000rpm, for various DC field current.

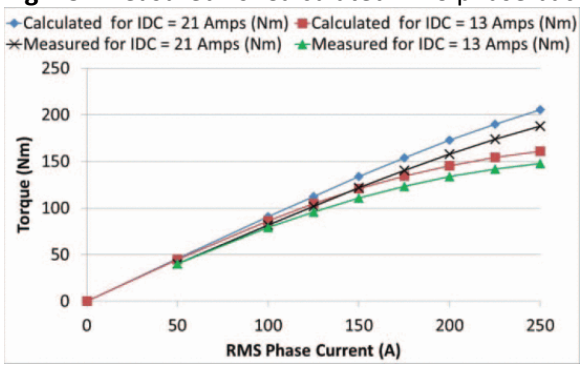

Fig. 20. Measured and calculated torque vs. Current for two levels of DC field current.

SECTION VI. Conclusion

Three different topologies of non-permanent magnet electrical machines were designed and compared for Electric/Hybrid vehicle traction: a conventional SRM, a DC-biased Reluctance Machine and a Wound Field Flux Switching Machine. The SRM uses a non-conventional half bridge inverter while the DCRM and WFFSM use a standard three phase inverter along with a DC/DC converter. The three designs were able to provide the required power within the required voltage and current limitations. Very smooth torque was achieved with the DCRM and the WFFSM but the best mass and efficiency was achieved with the conventional SRM. There were challenges related to the high frequency nature of the machines (2.3kHz to 2.8kHz fundamental frequency at 14000rpm):

- AC losses: Litz wire based on 33A WG was necessary for the armature winding, resulting in a lower copper fill factor.
- Iron losses: They become quickly dominant as the speed increases, requiring consideration of thinner laminations, particularly on the rotor.
- Efficiency: Challenging especially in the DCRM and WFFSM because of the additional copper losses in the field winding as well as the dominance of iron losses at higher speeds. Use of thin laminations (7mil or less) can improve the efficiency at high speed.

The choice of the machine topology for vehicle propulsion depends on the most important criteria for the application. Efficiency is one important criterion impacting the vehicle autonomy and favors the SRM in the present comparison. However, the significant torque ripple exhibited by the SRM may raise concern about noise and comfort. Also, the SRM requires a non-conventional inverter topology. The DCRM and WFFSM are alternatives with similar robustness but with lower efficiency and higher masses. They use a conventional three phase inverter and produce smooth torque, and possibly provide a better comfort than SRM. However, they use an additional DC/DC converter for the field winding which adds some degrees of complexity to the control.

A prototype of the DC biased Reluctance Machine was built and preliminary test results were in good accordance with predictions.

ACKNOWLEDGMENT

This material is based on work supported by the Department of Energy under Award Number: DE-E0005573.

References

1. T. Raminosoa, A. El-Refaie, D. Pan, K. Huh, J. Alexander, K. Grace, et al., "Reduced Rare-Earth Flux Switching Machines for Traction Applications", *Accepted for future publication in IEEE Transactions on Industry Applications*, pp. 13, 2015.
2. Steven Galioto, Patel Reddy and Ayman El-Refaie, "Effect of Magnet Types on Performance of High Speed Spoke Interior Permanent Magnet Machines designed for Traction Applications", *ECCE 2014*, September 14–18.
3. A. Chiba, K. Kiyota, N. Hoshi, M. Takemoto and S. Ogasawara, "Development of a Rare-Earth-Free SR Motor With High Torque Density for Hybrid Vehicles", *IEEE Transactions on Energy Conversion*, vol. 30, no. 1, pp. 175-182, March 2015.
4. A.M. Omekanda, "Switched reluctance machines for EV and HEV propulsion: State-of-the-art", *2013 IEEE Workshop on Electrical Machines Design Control and Diagnosis (WEMDCD)*, pp. 70-74, 2013.
5. X. Liu and Z.Q. Zhu, "Stator/Rotor Pole Combinations and Winding Configurations of Variable Flux Reluctance Machines", *IEEE Transactions on Industry Applications*, vol. 50, no. 6, pp. 3675-3684, November/December 2014.
6. R. Mikail, Y. Sozer, I. Husain, M. Islam and T. Sebastian, "Torque ripple minimization of switched reluctance machines through current profiling", *2011 IEEE Energy Conversion Congress and Exposition (ECCE)*, pp. 3658-3574, 2011.
7. K. Nakamura, Shinya Fujio and O. Ichinokura, "A Method for Calculating Iron Loss of an SR Motor Based on Reluctance Network Analysis and Comparison of Symmetric and Asymmetric Excitation", *IEEE Transactions on Magnetics*, vol. 42, no. 10, pp. 3440-3442, October 2006.